AGILE: GIScience Series, 3, 3, 2022. https://doi.org/10.5194/agile-giss-3-3-2022
Proceedings of the 25th AGILE Conference on Geographic Information Science, 2022.
Editors: E. Parseliunas, A. Mansourian, P. Partsinevelos, and J. Suziedelyte-Visockiene.
This contribution underwent peer review based on a full paper submission.

Optimizing Electric Vehicle Charging Schedules Based on Probabilistic Forecast of Individual Mobility

Haojun Cai[1], Yanan Xin[1], Henry Martin[1,2], and Martin Raubal[1]

[1]Institute of Cartography and Geoinformation, ETH Zurich, Zurich, Switzerland
[2]Institute of Advanced Research in Artificial Intelligence (IARAI), Vienna, Austria

Correspondence: Haojun Cai (caihao@ethz.ch)

Abstract. The number of electric vehicles (EVs) has been rapidly increasing over the last decade, motivated by the effort to decrease greenhouse gas emissions and the fast development of battery technology. This trend challenges distribution grids since EVs will bring significant stress if the charging of many EVs is not coordinated. Among the many strategies to cope with this challenge, next-day EV energy demand forecasting plays a key role. Existing studies have focused on predicting the next-day energy demand of EVs on the aggregated and individual levels. However, these studies have not yet extensively considered individual user mobility behaviors, which exhibit a high level of predictability. In this study, we consider several mobility features of individual users when forecasting the next-day energy demand of individual EVs. Three types of quantile regression models are used to generate probabilistic forecasts of energy demand, particularly the next-day energy consumption and parking duration. Based on the prediction results, two time-shifting smart charging strategies are designed: unidirectional and bidirectional smart charging. These two strategies are compared with an uncontrolled charging baseline to evaluate their financial benefits and peak-shaving effects. Our results show that human mobility features can partially improve the prediction of next-day individual EV energy demand. Additionally, users and distribution grids can benefit from smart charging strategies both financially and technically.

Keywords. smart charging, energy forecasting, individual mobility

1 Introduction

Smart charging enables us to adjust the charging schedules of electric vehicles (EVs) based on the needs of customers and the conditions of distribution grids to gain financial and technical benefits (García-Villalobos et al., 2014). When charging EVs, the electricity is transmitted from grids to vehicles. In addition, the electricity can be transmitted from vehicles to grids if vehicle-to-grid technology is utilized. To satisfy most mobility needs, EVs do not need to continue charging for a whole night or be fully charged to the maximum battery capacity when parked at home. Moreover, if a fleet of EVs is charged without any regulations, extra stress might be imposed on distribution grids. Therefore, it is crucial to deploy smart charging strategies that utilize the considerable time and energy flexibility of the charging processes. Such smart charging strategies include shifting charging schedules to off-peak with unidirectional control (e.g., Lopes et al., 2010; Sortomme and El-Sharkawi, 2010), time-shifting charging with bidirectional control (e.g., Restrepo et al., 2016; Al-Obaidi et al., 2021), and time-of-use pricing (e.g., Wei et al., 2016; Wu et al., 2020).

To enable the design and adoption of smart charging, we should acquire information about next-day energy demand particularly next-day energy consumption and parking duration, so that EVs can be charged flexibly to predicted energy consumption and in predicted parking duration. So far, existing research has focused on predicting energy demand on the aggregated level for EV fleets (Bessa and Matos, 2010; Kristoffersen et al., 2011; Sundstrom and Binding, 2011; Vandael et al., 2012), where a fixed driving pattern for each user is assumed. In reality, however, individual driving patterns differ. Though current research has studied predictions on individual EVs, limited attention has been paid to considering individual user mobility behaviors in prediction models. Nevertheless, studies have shown that individual human mobility has a considerably high level of predictability (Gonzalez et al., 2008; Song et al., 2010b; Pappalardo et al., 2015; Cuttone et al., 2018). As a result, our research focuses on how general mobility features can contribute to individual EV energy demand estimation in cases where detailed survey data of socio-demographics are hard to obtain.

This study takes the prediction of individual EV energy demand one step further to consider individual user mobility features in prediction models. The probabilistic models are chosen due to their ability to account for uncertainties. They provide the forecasting results and a measure of the certainty of the results. Both information can be used as inputs to design smart charging strategies. Our study focuses on several features to characterize individual user mobility patterns, including mobility entropy (Song et al., 2010b), the radius of gyration (Gonzalez et al., 2008; Yuan et al., 2012; Pappalardo et al., 2015, 2016), daily jump distance (Gonzalez et al., 2008), location frequency (Song et al., 2010a), and human mobility features related to EV usage.

We define our research question (RQ) as: To what extent can knowledge about individual user mobility help obtain monetary benefits and reduce charging peaks of electric vehicles? This question is further broken down into three sub-questions:

- **RQ 1.1**: To what extent can individual user mobility features help predict the next-day energy consumption?
- **RQ 1.2**: To what extent can individual user mobility features help predict the next-day parking duration?
- **RQ 1.3**: To what extent can next-day prediction help gain monetary benefits and achieve peak-shaving effects?

To answer RQ 1.1 and RQ 1.2, we first test the effects of individual user mobility features on the probabilistic prediction of next-day energy consumption and parking duration. Then, two time-shifting smart charging strategies are developed based on the prediction results and evaluated through a comparison with uncontrolled charging to solve RQ 1.3. This paper is structured as follows: Section 2 introduces the related work. Section 3 explains the methodology in detail, including the used data sets, data preprocessing, modeling methods, evaluation metrics, feature engineering, the design of charging strategies, and data and software availability. Section 4 presents the results of the prediction models, discusses the effects of individual user mobility features, and evaluates the financial and technical benefits of two smart charging strategies. Finally, Section 5 concludes the study and highlights future work.

2 Related Work

Smart Charging & Charging Infrastructures: For the last decade, research has focused on the optimization of EV charging strategies, named smart charging. Lopes et al. (2010) proposed a framework to manage and optimize the charging schedules of EV fleets. One typical smart charging strategy is to shift charging schedules to off-peak hours according to the electricity price (Lopes et al., 2010). Hu et al. (2011) proposed a framework for an optimal charging strategy and showed its effectiveness in reaching a minimum charging cost for users. Teng et al. (2020) presented a literature review about the participation of EVs in the electricity market. The study concluded that EVs could flexibly take part in the electricity market and provide technical benefits to distribution grids through the optimization of charging and discharging.

Our study simulates two smart charging strategies to investigate the effects of probabilistic predictions on smart charging from financial and technical perspectives as previous studies. First, we choose a typical form that shifts charging schedules to off-peak hours and another strategy that involves adding the step of vehicle-to-grid discharging in the typical form. The monetary gains for users and technical benefits to distribution grids are then evaluated. Home charging is set as the only charging scenario in our study. We base this decision on the study by Hardman et al. (2018), which reviewed different charging infrastructures and found that home charging is the most frequently used method in reality.

Energy Forecasting for Individual EVs: Forecasting energy demand for individual EVs offers high flexibility for customized control of smart charging operations and has drawn considerable attention from researchers (Xu et al., 2018; Huber et al., 2020; Hilpisch, 2020). Compared to these studies, our study provides a better understanding of how individual human mobility affects the energy demand forecasting for individual EVs.

First, we extract individual mobility features from a large set of high-resolution GPS tracking data rather than restricting the types of simulated travel patterns in Xu et al. (2018). That study incorporated individual user mobility patterns into the energy demand estimation of EVs. However, the used mobility data were simulated based on mobile phone data and two travel surveys. In addition, the used mobility features motifs characterize the daily regular travel network but omit non-typical individual travel behaviors.

Second, our prediction models use the location features from both EVs and EV users, and the data span nearly one year. Our research questions expand upon the work of Huber et al. (2020), in which probabilistic models mainly considered EV location features based on a one-week travel log. Their study concluded that the improvement of including location features is significant; however, it was relatively low. Future work suggests that the prediction accuracy might increase if user trip trajectories are utilized in the prediction (Huber et al., 2020).

Third, our prediction models not only consider individual user mobility features but also train a model for each individual to capture individual variabilities, building on the work by Hilpisch (2020). His study predicted next-day EV energy demand and parking duration based only on the EV car data set used in our study, and his study trained one prediction model for all users. His results showed that not all models outperformed the benchmark that used the mean values of previous targets. Our work builds on the suggestion that individual user behavior can be incorporated to further improve predictions (Hilpisch, 2020).

All three previous studies pointed to the need to incorporate individual user mobility behavior more comprehensively into EV demand forecasting. Thus, our study considers commonly-used human mobility features to predict individual EV energy demand.

Individual Mobility: Individual mobility has predictability from past regular activities while also possesses uncertainty because of irregular behaviors. Song et al. (2010b) introduced mobility entropy measures by considering visitation frequency and the series of visited locations. They tested the entropy features for 50,000 individuals on three-month call detail records and found an overall 93% potential predictability. Gonzalez et al. (2008) proposed the radius of gyration that models the characteristic traveling distance by an individual. A high level of spatial and temporal regularity was found by testing 100,000 anonymized mobile phone users for half a year. Yuan and Raubal (2016) comprehensively studied the human mobility patterns from both mobility entropy and the radius of gyration using nine-day call detail records. Additionally, other individual measures help to depict individual mobility patterns such as traveled distance between consecutive visited locations (Gonzalez et al., 2008) and the frequency of visited locations (Song et al., 2010a). All above-mentioned mobility features can measure individual traveling behaviors showing a level of predictability and are therefore considered in our prediction models. In addition, we also consider the share of EV usage among all transport modes, which is modeled using a variant of the Herfindahl–Hirschman Index (HHI) (Rhoades, 1993). The HHI score is often used to quantify the concentration ratio of members and has recently been widely used in quantifying dominance or variability of mode choices (Susilo and Axhausen, 2014; Hong et al., 2021).

3 Method

3.1 Data Introduction

Our study utilizes a long-term tracking data set collected through a pilot project by the Swiss Federal Railways (SBB) (Martin et al., 2019; Bucher et al., 2020). Over one hundred participants took part in the project from November 2016 to December 2017. Each participant was provided with a battery EV of 27.2 kWh usable battery capacity, and a volt box was installed at home to charge EVs with a rated power of 11 kW. Besides, a first-class Swiss travel pass for public transportation and access to car-sharing and bike-sharing services were provided. Moreover, most participants have one or multiple internal combustion engine vehicles themselves. During the project, the mobility of participants was recorded using a GPS-tracking application that was installed on their mobile phones. The users provided labels for the used mode of transport and labeled each visited location as one of the categories including home, work, errand, leisure, wait, and unknown (Martin et al., 2019). This data set is referred to as user data in our study. In addition, EV-related information such as battery status, locations, and timestamps was collected from the sensors installed in the car, referred to as car data. Besides, we use Swiss electricity spot prices during the same period as the SBB data and a publicly available standard load profile for households in Germany as an approximation for Switzerland. Usually, EVs can collect car data with sensors installed in the car, whereas user data requires extra effort to collect. By answering how much human mobility features can help EV predictions, relevant stakeholders can better decide if it is worthwhile to put extra effort into collecting human mobility data.

3.2 Data Preprocessing

First, we only keep the overlapping period of car data and user data from February 2017 to December 2017. Second, 22 users are omitted due to a lack of valid records labeled as home, resulting in 113 final users for this study. Third, since the provided user data has been preprocessed to stay points, we cluster them to locations using the density-based spatial clustering of applications with noise (DBSCAN) method (Ester et al., 1996). Two key parameters, search radius ϵ and the minimum number of samples per cluster $\mathrm{min\_samples}$, are respectively set as $\epsilon = 100$ m and $\mathrm{min\_samples} = 1$, basing on the manual inspection of the clustering results. The DBSCAN returns an average of 504 visited locations per user.

3.3 Modeling Next-Day Energy Demand

The problem of predicting next-day energy demand is split into two tasks: next-day energy consumption and next-day parking duration. Probabilistic forecasts are chosen since they can account for uncertainty in real-life scenarios (Huber et al., 2020; Hilpisch, 2020). Unlike point forecasts which output definite target values, probabilistic forecasts return the distribution of target values. As a result, they are chosen to predict next-day EV energy demand in our study to account for the uncertainties of travel behaviors. In most cases, they predict a set of quantiles to approximate the probability distribution. As defined in Eq. 1, the quantile regression models return the conditional quantile result Q_α for a given input probability α, so that the probability of the true value y lying below the given predicted result Q_α will be the specified input probability α:

$$\Pr(y < Q_\alpha) = \alpha, 0 \leq \alpha \leq 1. \quad (1)$$

Therefore, the quantile prediction returns results based on not only given observations but also input probability. Our study uses three quantile prediction models: linear quantile regression, quantile random forest, and gradient boosting quantile regression. Koenker and Bassett (1978) introduced linear quantile regression that is more robust to non-Gaussian distributed data, which extends the ordinary least-squares regression by returning the conditional quantile of given observations instead of the conditional mean. Besides, it can be easily interpreted. Furthermore, the quantile regression can be combined with other modeling methods like decision-tree-based methods returning quantile random forest and gradient boosting quantile regression (Meinshausen and Ridgeway, 2006). They are chosen due to their overall good performance and robustness to hyperparameter tuning.

3.4 Model Performance Metrics

Mean absolute error is used to evaluate the general accuracy of model predictions. In addition, two evaluation metrics specific to quantile regression are used: (1) mean quantile loss, (2) the pair of outbound ratio and average inbound range.

3.4.1 Mean Absolute Error

Mean absolute error (MAE) is a measure between true values and predictions, which is defined as below:

$$\mathrm{MAE} = \frac{\sum_{i=1}^{n} |Q_\alpha - y|}{n}, \tag{2}$$

where Q_α is the predicted value and y is the true value.

3.4.2 Mean Quantile Loss

The standard loss function of quantile prediction is quantile loss L_α, also called pinball loss (Meinshausen and Ridgeway, 2006), which is defined as follows:

$$L_\alpha = \begin{cases} \alpha|y - Q_\alpha|, & y > Q_\alpha, \\ (1-\alpha)|y - Q_\alpha|, & y \le Q_\alpha. \end{cases} \tag{3}$$

For each quantile regression, the mean quantile loss is calculated over all specified input quantiles and all users.

3.4.3 Outbound Ratio and Average Inbound Range

Based on quantile results, we can calculate the central prediction interval such that the probability of the true value lying in the interval is $x\%$, called $x\%$ prediction intervals (Zhou et al., 2010; Wang and Lee, 2019). Given a user i on a day j ($j \in \{1, 2, \cdots, d_i\}$),

$$x\% \text{ prediction interval} = [Q_{ij,\alpha^-},\ Q_{ij,\alpha^+}],$$
$$\alpha^- = \frac{100-x}{2}\%,\ \alpha^+ = (100 - \frac{100-x}{2})\%. \tag{4}$$

Fig. 1 illustrates the relationships between true values and prediction intervals. Outbound ratio calculates the percentage of outbound cases when true values are outside prediction intervals. The average inbound range returns the mean values of prediction intervals for inbound cases (Hilpisch, 2020). The outbound ratio and average inbound range are a pair of trade-offs, and they must be reported together to evaluate models. In general, with increasing $x\%$ prediction intervals, there will be a smaller outbound ratio and a larger average inbound range. A pair of a smaller outbound ratio and a narrower average inbound range indicates a better performance. In reality, it is essential to check if true values lie in prediction intervals. A model gives minimal value if most predicted intervals do not contain true values, even with the smallest mean quantile loss.

3.5 Feature Engineering

Table 1 presents all target and input features. All features are first extracted per day. Then, human mobility and EV-related input features are averaged over the past three days.

3.5.1 Target Features

For next-day energy consumption prediction, the target is the daily consumed state of charge (SoC); SoC describes the percentage of available battery capacity in EVs. The daily SoC consumption $\mathrm{SoC}_{\mathrm{day}_i}$ can be calculated by summing up all records whose SoC status are decreased. Parking duration can be regarded as the period from arrival time on one day to the departure time the next day. Therefore, the prediction of parking duration is formulated as predicting the arrival and departure time in our study. As a result, there are three forecasting targets: SoC consumption, arrival time, and departure time.

3.5.2 Input Features

Our study uses four types of input features, temporal, historical, EV-related, and human mobility features. Weekday information from Monday to Sunday and weekend flag indicating if one day is on the weekend or not are two chosen temporal features for three predictions. SoC consumption, arrival time, and departure time in the previous three individual days are used as historical features respectively. For SoC prediction, two EV-related features are utilized:

1. EV traveling distance $D_{EV\,1,n} = d_{EV\,1,2} + d_{EV\,2,3} + \cdots + d_{EV\,n-1,n}$ is the daily traveling distance by EVs between consecutive locations.
2. EV traveling duration $T_{EV\,1,n} = t_{EV\,1,2} + t_{EV\,2,3} + \cdots + t_{EV\,n-1,n}$ is the daily traveling duration by EVs between consecutive locations.

The features mentioned above are extracted from car data, whereas the following human mobility features are calculated from user data.

1. Real entropy $S = -\sum_{T' \subset T} p_{T'} \log_2 p_{T'}$ describes the predictability of an individual's whereabouts which considers visitation frequency of each location and the order of visited locations. T is the sequence of all

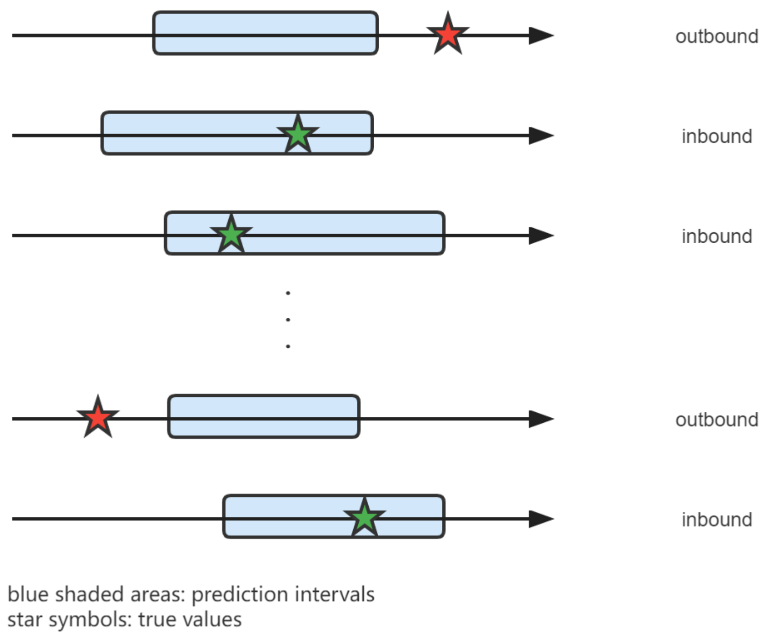

Figure 1. Inbound and outbound relationships between true values and prediction intervals.

visited locations, T' runs over all time-ordered subsequences of T, and $p_{T'}$ calculates the probability of a visit sequence T' (Song et al., 2010b).

2. Top-3 location visitation frequency $p_{top_3} = \frac{n_{top_3}}{N}$ returns visitation frequency to the most frequently-visited three locations, where n_{top_3} is the number of visits to the most frequently-visited three locations, and N is the total number of visits to all locations.
3. Average jump distance $\overline{D_{1,n}} = \frac{d_{1,2}+d_{2,3}+\cdots+d_{n-1,n}}{n}$ is the daily average traveling distance between consecutive locations visited by an individual (Gonzalez et al., 2008).
4. Radius of gyration $r_g = \sqrt{\frac{1}{N}\sum_{i\in L} n_i(r_i - r_{cm})^2}$ describes the typical distance traveled by an individual. N is the total number of visits, n_i is the number of visits to location i, L is the set of all visited locations, r_i is the geographical coordinates of location i, and r_{cm} are the geographical center of all locations (Gonzalez et al., 2008).

Additionally, one more human mobility feature is extracted for SoC prediction:

1. EV HHI score $HHI_{EV} = \frac{Share_{EV}^2}{\sum_{m\in mode} Share_m^2}$ depicts daily EV usage among all transport modes (Rhoades, 1993; Susilo and Axhausen, 2014; Hong et al., 2021). $Share_m = \frac{D_m}{\sum_{m\in mode} D_m}$ and D_m is the traveling distance by a mode in the following categories:

   mode ={airplane, bicycle, boat, bus, car, coach, e-bicycle, e-car, ski, train, tram},

where e-car is an interchangeable term with EV, and car denotes internal combustion engine vehicles.

3.6 Charging Strategy Design

We choose two representative smart charging strategies with simplified design under the following assumptions:

1. Only overnight home charging is considered given that home charging is most frequently used (Hardman et al., 2018; Mwasilu et al., 2014).
2. Electricity spot prices are known to guide the trading of electricity and optimization of charging schedules.

In practice, energy consumption, arrival time, and departure time can be forecasted one day in advance when EV car and EV user data are available. Smart charging can then be deployed following the forecast. Generally, it is risky to underestimate energy consumption and overestimate parking duration. An underestimation of energy consumption can potentially jeopardize users' travel needs. An overestimation of parking duration may recommend charging times when EVs are not at home, resulting in a failure to charge EVs. Thus, to reasonably evaluate the effects of probabilistic predictions on smart charging, we use the predicted energy consumption with input quantile $\alpha \geq 0.5$ and the predicted parking duration with $\alpha \leq 0.5$, whose details are given in Section 4.2.

Table 1. Input and target features for SoC consumption, arrival time, and departure time predictions.

Feature	Type	Coding	Category of Features	Usage of Predictions
Weekday on the predicting day	Ordinal	$\{0, 1, 2, 3, 4, 5, 6\}$	Input (temporal)	SoC, Arrival, Departure
Weekend flag on the predicting day	Nominal	{weekday, weekend}	Input (temporal)	SoC, Arrival, Departure
SoC in the previous day	Ratio	$[0, 100]$	Input (historical)	SoC
SoC two days ago	Ratio	$[0, 100]$	Input (historical)	SoC
SoC three days ago	Ratio	$[0, 100]$	Input (historical)	SoC
Arrival time in the previous day	Ratio	$[0, 24]$	Input (historical)	Arrival
Arrival time two days ago	Ratio	$[0, 24]$	Input (historical)	Arrival
Arrival time three days ago	Ratio	$[0, 24]$	Input (historical)	Arrival
Departure time in the previous day	Ratio	$[0, 24]$	Input (historical)	Departure
Departure time two days ago	Ratio	$[0, 24]$	Input (historical)	Departure
Departure time three days ago	Ratio	$[0, 24]$	Input (historical)	Departure
Average EV distance over past three days	Ratio	$[0, \infty)$	Input (EV-related)	SoC
Average EV duration over past three days	Ratio	$[0, 86400]$	Input (EV-related)	SoC
Average real entropy over past three days	Ratio	$[0, \infty)$	Input (human mobility)	SoC, Arrival, Departure
Average top-3 location visitation frequency over past three days	Ratio	$[0, 1]$	Input (human mobility)	SoC, Arrival, Departure
Average jump distance over past three days	Ratio	$[0, \infty)$	Input (human mobility)	SoC, Arrival, Departure
Average radius of gyration over past three days	Ratio	$[0, \infty)$	Input (human mobility)	SoC, Arrival, Departure
Average EV HHI score over past three days	Ratio	$[0, 1]$	Input (human mobility)	SoC
Next-day SoC	Ratio	$[0, 100]$	Target	SoC
Next-day arrival time	Ratio	$[0, 24]$	Target	Arrival
Next-day departure time	Ratio	$[0, 24]$	Target	Departure

3.6.1 Uncontrolled Charging

We use uncontrolled charging as a baseline, when EVs are charged as soon as users arrive home and to the maximum battery capacity. It consists of two steps, charging and using EVs. In Step 1, the SoC of EVs will be charged to the maximum level 100%. In Step 2, users will consume exact amount of energy as in reality. The daily financial costs are calculated using the hourly prices during charging slots and then the total costs over the collection period are returned for each user. Hourly charging energy is recorded for the comparison of peak-shaving effects. For each user, Step 1 and Step 2 are iterated over the period when there are valid SoC consumption and parking duration.

- Step 1–Charge EV:

$$\mathrm{SoC_{end}}(\mathrm{day}_i) + \mathrm{SoC_{charge}}(\mathrm{day}_i) = \mathrm{SoC_{start}}(\mathrm{day}_{i+1}) = 100$$

- Step 2–Use EV:

$$\mathrm{SoC_{start}}(\mathrm{day}_{i+1}) - \mathrm{SoC_{diff_{true}}}(\mathrm{day}_{i+1}) = \mathrm{SoC_{end}}(\mathrm{day}_{i+1})$$

3.6.2 Unidirectional Smart Charging

Unidirectional smart charging considers the unidirectional electricity flow from grids to vehicles. It shifts charging schedules to off-peak hours which are decided based on the electricity spot prices, and EVs are charged by the amount of predicted energy consumption. Step 2 is the same as in the uncontrolled charging strategy, but $\mathrm{SoC_{end}}(\mathrm{day}_{i+1})$ will be reset as 0 if it ends below 0. The time needed to charge the difference between 0 and $\mathrm{SoC_{end}}(\mathrm{day}_{i+1})$ using the same rated power is regarded as the risk of charging outside the home. Step 1 is different from uncontrolled charging, as here the total amount of charged energy is the predicted energy consumption, and the charging schedules are arranged during off-peak hours in the predicted parking duration when the prices are most favorable. The total costs over the period and hourly charging energy are returned similarly as in uncontrolled charging for the comparison.

Step 1–Charge EV:

$$\mathrm{SoC_{end}}(\mathrm{day}_i) + \mathrm{SoC_{uni\_charge}}(\mathrm{day}_i) = \mathrm{SoC_{start}}(\mathrm{day}_{i+1})$$

3.6.3 Bidirectional Smart Charging

Bidirectional smart charging considers bidirectional electricity flow from grids to vehicles and vehicles to grids, assuming vehicle-to-grid (V2G) technology is utilized. In this way, the remaining energy of EVs can be discharged back to distribution grids. The bidirectional smart charging follows the same Step 1 and Step 2 as the unidirectional scenario. In addition, one more step is added before charging EVs. In Step 0, from arrival time till the start of charging, we assume users do not need EVs anymore so all remaining energy can be sold to distribution grids. This is a simple design of V2G; nevertheless, it serves to demonstrate the potential benefits of integrating V2G into unidirectional charging. Under this assumption, the $\mathrm{SoC_{end}}(\mathrm{day}_i)$ ends at a low value or even 0%. Corresponding gains are calculated by picking up the most favorable prices. Therefore, the daily financial costs are returned as grid-to-vehicle costs minus vehicle-to-grid gains.

Step 0–Discharge EV: $\mathrm{SoC_{end}}(\mathrm{day}_i) = 0$, if all left energy is sold by the time of Step 1 starts.

3.7 Data and Software Availability

EV car data and user data cannot be made available due to the non-disclosure agreement with participants. Electricity spot prices are available for purchase from EPEX Spot[1], and standard load profile data is accessible for free online[2].

The implementation of data processing, smart charging simulation, and charging strategy evaluation is accessible at a GitHub repository[3]. We use Python packages of scikit-learn, statsmodels, scikit-garden for probabilistic modeling, and geopandas and trackintel to process data.

4 Results and Discussion

In this section, we discuss the model performances of linear quantile regression (LQR), quantile random forest (QRF), and gradient boosting quantile regression (GBQR) for SoC consumption, arrival time, and departure time predictions. Prediction models are trained by including and excluding human mobility features respectively to examine their impact on the predictions. Furthermore, the models are trained for each user to capture individual variabilities, and only days with valid targets are fed into the models. In addition, the evaluation of smart charging strategies from financial and technical aspects is presented.

4.1 Model Evaluation

Quantile predictions at $\alpha = [0.025, 0.05, \cdots, 0.95, 0.975]$ are returned in our study. Data are split by time series so that the first 75% is used for training and the remaining 25% for testing. Five-fold cross validation is applied to each model to find the optimal hyperparameters (the details of search spaces are given in Appendix A).

To evaluate predictability, the mean absolute error is returned. For probabilistic predictions, mean quantile loss is calculated over all probabilities and all users. The smaller the mean quantile loss is, the better the model performs. The pair of outbound ratio and average inbound range are averaged for all users at three chosen levels: 95%, 90%, and 70% prediction intervals. A model can be concluded to have a good performance if the outbound ratio and average inbound range are both small.

4.1.1 Mean Absolute Error

Table 2 presents the mean absolute error (MAE) of quantile predictions at the median. Overall, there is around 16% MAE for SoC prediction and 3 hours MAE for arrival time or departure time predictions.

[1]https://www.epexspot.com/en/market-data

[2]https://www.ggv-energie.de/cms-wAssets/docs/stadt/netz/netzbilanzierung/download-aller-profile/GGV_SLP_1000_MWh_2021_01-2020-09-24.xlsx

[3]https://github.com/HaojunCai/agile22_evprediction

Table 2. Mean absolute error of next-day SoC consumption, arrival time, and departure time median predictions (SoC Unit: %, Arrival and Departure Unit: hours).

Model	SoC	Arrival	Depart
LQR	15.9413	3.5631	3.0417
LQR+Mobility	16.4257	3.5595	2.9793
QRF	16.2367	3.1701	3.0603
QRF+Mobility	16.3325	3.0499	2.9752
GBQR	15.9135	3.0842	2.9448
GBQR+Mobility	16.007	3.0909	2.9499

4.1.2 Mean Quantile Loss

Table 3 gives the mean quantile loss of three targets. Quantile random forest with human mobility features performs best for all three targets. As for human mobility features, they help improve the model performance of quantile random forest for all three targets and linear quantile regression for departure time prediction. However, the mobility features have a negative impact on linear quantile regression for SoC predictions, probably because EV HHI scores are highly correlated with EV traveling distance and duration, which cannot be dealt with well by the model.

Table 3. Mean quantile loss of next-day SoC consumption, arrival time, and departure time predictions (SoC Unit: %, Arrival and Departure Unit: hours). A smaller value indicates a better performance. The model with the best performance is highlighted in bold, and models that perform better after including human mobility features are underlined.

Model	SoC	Arrival	Departure
LQR	6.0231	1.3806	1.1759
<u>LQR+Mobility</u>	6.1838	1.3923	<u>1.1668</u>
QRF	5.9571	1.2048	1.1859
<u>**QRF+Mobility**</u>	<u>**5.9544**</u>	<u>**1.1705**</u>	<u>**1.1499**</u>
GBQR	6.0036	1.1873	1.1587
GBQR+Mobility	6.0416	1.1902	1.162

4.1.3 Outbound Ratio and Average Inbound Range

Table 4 presents the pairs of outbound ratio and average inbound range for three targets at 95%, 90%, and 70% prediction intervals. Quantile random forest and gradient boosting quantile regression outperform linear quantile regression since the outbound ratio and average inbound range are generally smaller. For arrival and departure time predictions, the best model of 70% prediction intervals is the quantile random forest with human mobility features since it has the smallest outbound ratio and the narrowest average inbound range, whereas the best model is not found for others. With human mobility features, better model performance is observed for 70% prediction intervals of quantile random forest when predicting arrival and departure time and for 95%, 90%, and 70% prediction intervals of gradient boosting quantile regression when predicting departure time.

Table 4. Outbound ratio and average inbound range for next-day SoC consumption, arrival time, and departure time predictions at 95%, 90%, and 70% prediction intervals. A simultaneous smaller outbound ratio and narrower averaged inbound range indicate a better model performance. Models with the best performance are highlighted in bold, and models that perform better after including human mobility features are underlined.

Target	Model	Outbound Ratio [%]			Average Inbound Range [SoC: %, Arrival & Departure: hours]		
		95%	90%	70%	95%	90%	70%
SoC	LQR	11.17	15.55	34.73	70.05	61.16	37.88
	LQR+Mobility	14.89	18.50	35.99	66.98	58.83	37.29
	QRF	2.38	3.76	8.44	57.66	46.76	24.38
	QRF+Mobility	2.08	3.40	8.07	59.19	48.07	24.52
	GBQR	7.03	13.74	34.93	63.22	50.44	27.38
	GBQR+Mobility	7.19	13.59	34.88	63.34	51.37	28.06
Arrival	LQR	9.26	14.43	34.20	17.11	14.15	8.04
	LQR+Mobility	10.46	15.52	35.21	16.56	13.82	8.00
	QRF	5.38	6.91	11.58	11.55	9.12	4.71
	QRF+Mobility	3.92	5.33	**10.00**	12.17	9.47	**4.68**
	GBQR	8.38	14.24	34.59	13.25	10.38	5.28
	GBQR+Mobility	8.17	14.40	34.87	13.46	10.22	5.08
Departure	LQR	7.25	11.77	30.54	15.29	12.33	6.54
	LQR+Mobility	8.86	13.31	32.01	14.86	12.10	6.38
	QRF	5.48	6.87	11.56	10.59	8.37	4.33
	QRF+Mobility	3.85	4.95	**9.35**	11.13	8.67	**4.27**
	GBQR	5.57	11.63	32.39	15.67	11.34	5.26
	GBQR+Mobility	5.51	11.50	32.33	15.64	11.31	5.09

4.1.4 Human Mobility Features Evaluation

Feature importance returned by quantile random forest with human mobility features is presented in Table 5. Energy consumption and parking duration in the past three individual days help the predictions in general; however, human mobility features do not rank at the top.

Five human mobility features chosen in our study are believed to help to predict next-day EV energy demand since they can depict the mobility behaviors of EV owners. This belief relies on the assumption that EV usage is relatively stable among all transportation choices so that the mobility features can be descriptors for EV usage. However, the EV usage is not stable as indicated by daily EV HHI scores. This mobility metric quantifies the concentration of daily EV usage among all transport modes. The value ranges from 0 to 1, with 0 meaning no EV usage and 1 meaning pure EV usage. The average standard deviation of EV HHI scores for all users is 0.348, indicating that participants in the SBB project do not have consistent habits towards EV usage. Besides, the other four mobility features do not distinguish mode choices and therefore have limited contribution to predicting next-day EV energy demand for our participants. The human mobility features can potentially play a more important role when forecasting the EV demand of users who mainly use EVs for traveling or have a stable EV mode share.

Regarding arrival and departure time predictions, an additional reason for the marginal contribution of human mobility features is that these two targets are not strongly related to chosen mobility features. These features mainly describe mobility behaviors from the spatial perspective, with limited information on the temporal perspective.

4.2 Charging Strategy Evaluation

This section presents the financial benefits and peak-shaving effects of two smart charging scenarios compared to uncontrolled charging. The prediction results of quantile random forest with human mobility features are used because of its overall good and robust performance.

As mentioned in Section 3.6, it is of higher risk to underestimate SoC and overestimate parking duration. The worst case of overestimating parking duration is to have the underestimation of arrival time and the overestimation of departure time. However, the total time to charge an EV in our project is around 2.5 hours (2.5 hours $\approx$ 27.2 kWh $\div$ 11 kW). Considering the parking duration usually lasts a whole night, the uncertainty of predicted parking duration has a smaller impact on charging strategies than the predicted energy consumption. Therefore, arrival predictions at $\alpha = 0.9$ and departure predictions at $\alpha = 0.1$ are chosen so that there is only a 10% chance of EVs arriving home later than the predicted arrival time and departing home earlier than the predicted departure time. For energy consumption, prediction results at $\alpha = [0.5, 0.55, 0.6, 0.65, 0.7, 0.75, 0.8, 0.85, 0.9, 0.95]$ are used to test the impacts of different quantile predictions on smart charging. Additionally, we only consider days with valid energy consumption and parking duration. For all 113 users, 237 days are kept on average.

Table 5. Mean importance returned by QRF+Mobility for next-day SoC consumption, arrival time, and departure time predictions. The top three ranked features are in bold.

Feature	SoC	Arrival	Departure	Category of Features
Weekday on the predicting day	0.08	**0.12**	**0.15**	Input (temporal)
Weekend flag on the predicting day	0.02	0.02	0.05	Input (temporal)
SoC/Arrival/Departure in the previous day	**0.11**	**0.16**	**0.16**	Input (historical)
SoC/Arrival/Departure two days ago	**0.10**	**0.13**	0.11	Input (historical)
SoC/Arrival/Departure three days ago	**0.10**	**0.13**	**0.12**	Input (historical)
Average EV distance over past three days	0.09	-	-	Input (EV-related)
Average EV duration over past three days	0.09	-	-	Input (EV-related)
Average real entropy over past three days	0.09	0.12	0.11	Input (human mobility)
Average top-3 location visitation frequency over past three days	0.09	0.11	0.11	Input (human mobility)
Average jump distance over past three days	0.08	0.11	0.10	Input (human mobility)
Average radius of gyration over past three days	0.08	0.10	0.10	Input (human mobility)
Average EV HHI score over past three days	0.06	-	-	Input (human mobility)

4.2.1 Financial Benefits

The total financial cost for a fleet of 113 EVs over 237 days of uncontrolled charging strategy is 8491 € by summing up daily monetary costs over all users and all days. For per user, total costs over 237 days are 75 €. With input SoC predictions at different probabilities, Table 6 presents the risks per user per day and total financial costs per user over 237 days of unidirectional and bidirectional smart charging strategies and their benefit ratios compared to the uncontrolled charging. The risk is the time needed to charge EVs outside the home when EVs run out of batteries. The benefit ratio, calculated as the benefits of smart charging divided by the cost of uncontrolled baseline, is given as a more informative metric than the benefits since our study uses electricity spot prices that differ a lot compared to customer prices in practice.

As shown in Table 6, both unidirectional and bidirectional smart charging strategies can help users save more money than uncontrolled charging. In unidirectional smart charging, the risk and the total benefit decrease as the input probability of SoC predictions increases since increasing energy is charged at home. There is a trade-off between risks and monetary benefits: using a more conservative strategy to charge EVs, less benefit is gained while less risk is undertaken. Moreover, with input probability α decreasing, the risk and benefit slowly increase until α goes below 0.65. For each user, SoC predictions with $\alpha \geq 0.70$ can guarantee no more than 12 minutes' charging outside the home every day and a 29.8% monetary benefit ratio for 237 days.

For bidirectional smart charging, the risk decreases and the total benefit increases when the quantile of SoC predictions increases, because the energy demand with a larger input probability will result in a higher amount of remaining energy to be sold for V2G. However, this selling step, on the one hand, brings higher risks compared to unidirectional charging since SoC is either 0 or very low after selling energy, leaving a small buffer if the predicted next-day energy demand is lower than the true consumption. On the other hand, unexpected EV needs from users might not be fulfilled after they arrive home because of this discharging procedure. For each user, SoC predictions with $\alpha \geq 0.85$ guarantee less than 30 minutes' charging outside the home and a 50% monetary benefit ratio for 237 days.

4.2.2 Peak-Shaving Effects

The maximum electricity load is compared between uncontrolled charging and two smart charging scenarios to evaluate peak-shaving effects. The standard load profile is normalized to 113 families. The highest peak demand $\mathrm{MaxLoad_{ori}}$ of original household is 445.0 kW. When charging 113 electric vehicles at home using the uncontrolled charging, the maximum peak load $\mathrm{MaxLoad_{base}}$ reaches 518.1 kW with an increase of 73.1 kW, which is not beneficial for grid stability. Table 7 presents the maximum electricity load with 113 EVs charged using unidirectional and bidirectional smart charging and their increase compared to the original peak demand $\mathrm{MaxLoad_{ori}}$. According to Table 7, unidirectional smart charging at all quantiles and bidirectional smart charging with $\alpha \leq 0.65$ will not increase the original maximum peak load, whereas uncontrolled charging will bring an increase of 73.1 kW.

Fig. 2 shows the hourly load profile of the original household and the total load of the original household plus EV charging from three charging strategies with SoC predictions at 0.75 quantile. As shown in Fig. 2, the charging processes of EVs in the unidirectional (green line) and bidirectional smart charging (yellow line) mainly occur when the original household demand (black line) is relatively low. On the contrary, the uncontrolled charging of EVs (blue line) happens mainly during the high-demand hours of the original household. Moreover, the original maximum peak demand at 8 p.m. is even decreased in bidirectional smart charging because of the discharging arrangement. Although it induces a new maximum peak at 4 a.m., this induced peak can be evened out by adopting a more advanced V2G design since our design is rather simple.

Table 6. Risks and monetary benefits of unidirectional and bidirectional smart charging and their benefit ratios compared to uncontrolled charging with SoC prediction (QRF+Mobility) at different quantiles (Risk in hours:minutes:seconds, Benefit Unit: €).

The Quantile of	Unidirectional			Bidirectional		
SoC Prediction	$\mathrm{Risk}_{\mathrm{uni}}$	$\mathrm{Benefit}_{\mathrm{uni\_base}}$	$\mathrm{Benefit\_Ratio}_{\mathrm{uni\_base}}$	$\mathrm{Risk}_{\mathrm{bi}}$	$\mathrm{Benefit}_{\mathrm{bi\_base}}$	$\mathrm{Benefit\_Ratio}_{\mathrm{bi\_base}}$
0.50	1:05:46	28.4	37.9%	1:44:21	31.3	41.3%
0.55	0:46:49	26.9	35.8%	1:29:56	31.4	41.7%
0.60	0:30:47	25.5	34.1%	1:16:23	31.7	42.2%
0.65	0:18:53	24.5	32.7%	1:03:44	32.1	42.8%
0.70	0:11:41	23.8	31.7%	0:53:22	32.6	43.4%
0.75	0:07:15	23.3	31.1%	0:44:20	33.8	45.1%
0.80	0:04:35	23.0	30.6%	0:35:17	36.1	48.1%
0.85	0:03:00	22.7	30.2%	0:26:25	39.7	53.0%
0.90	0:01:41	22.5	30.0%	0:17:38	45.8	61.0%
0.95	0:00:32	22.4	29.8%	0:09:16	56.1	74.8%

Table 7. Maximum electricity load of unidirectional and bidirectional smart charging and their increase compared to the maximum electricity load of the original household with SoC prediction (QRF+Mobility) at different quantiles (Unit: kW).

The Quantile of	Unidirectional		Bidirectional	
SoC Prediction	$\mathrm{MaxLoad}_{\mathrm{uni}}$	$\mathrm{MaxLoad\_diff}_{\mathrm{uni\_ori}}$	$\mathrm{MaxLoad}_{\mathrm{bi}}$	$\mathrm{MaxLoad\_diff}_{\mathrm{bi\_ori}}$
0.50	445.0	0.0	435.0	-10.0
0.55	445.0	0.0	432.5	-12.5
0.60	445.0	0.0	430.3	-14.7
0.65	445.0	0.0	443.3	-1.7
0.70	445.0	0.0	461.4	16.4
0.75	445.0	0.0	486.0	41.0
0.80	445.0	0.0	520.4	75.4
0.85	445.0	0.0	562.8	117.8
0.90	445.0	0.0	628.9	183.8
0.95	445.0	0.0	730.2	285.2

5 Conclusion and Future Work

With increasing EVs on the road, it is crucial to deploy charging strategies wisely for the benefit of EV owners and distribution grids. The deployment of smart charging requires accurate information about next-day energy demand. Our study explores whether individual user mobility features can help the probabilistic prediction of next-day energy consumption and parking duration, and how prediction results can benefit time-shifting smart charging strategies considering V2G technology. Our research questions in Section 1 are answered as follows.

- **RQ 1.1**: To what extent can individual user mobility features help predict the next-day energy consumption?

  Individual user mobility features partially help the probabilistic prediction of next-day energy consumption. Specifically, the performance of quantile random forest is improved marginally after including human mobility features from mean quantile loss.

  Marginal improvements appear mainly due to the inconsistent EV usage habits of participants in our study, which render the human mobility features less effective in estimating EV demand. Nevertheless, in cases where traveling needs are mainly fulfilled by EVs, human mobility features should contribute more to the prediction of next-day energy consumption.

- **RQ 1.2**: To what extent can individual user mobility features help predict the next-day parking duration?

  Individual user mobility features partially help the probabilistic prediction of next-day arrival and departure time. Specifically, for arrival time predictions, quantile random forest performs better after including human mobility features from the mean quantile loss; from the outbound ratio and average inbound range, quantile random forest at 70% prediction intervals performs better with human mobility features.

  For departure time predictions, with human mobility features, linear quantile regression and quantile random forest perform better from mean quantile loss; from the outbound ratio and average inbound range, better performance is found for the 70% prediction interval of quantile random forest and the 95%, 90%, 70% prediction intervals of gradient boosting quantile regression.

  In addition to the explanation in RQ 1.1, another reason for partial improvements is that the chosen mobility features in our study depict traveling habits from the spatial perspective with limited information on the temporal perspective.

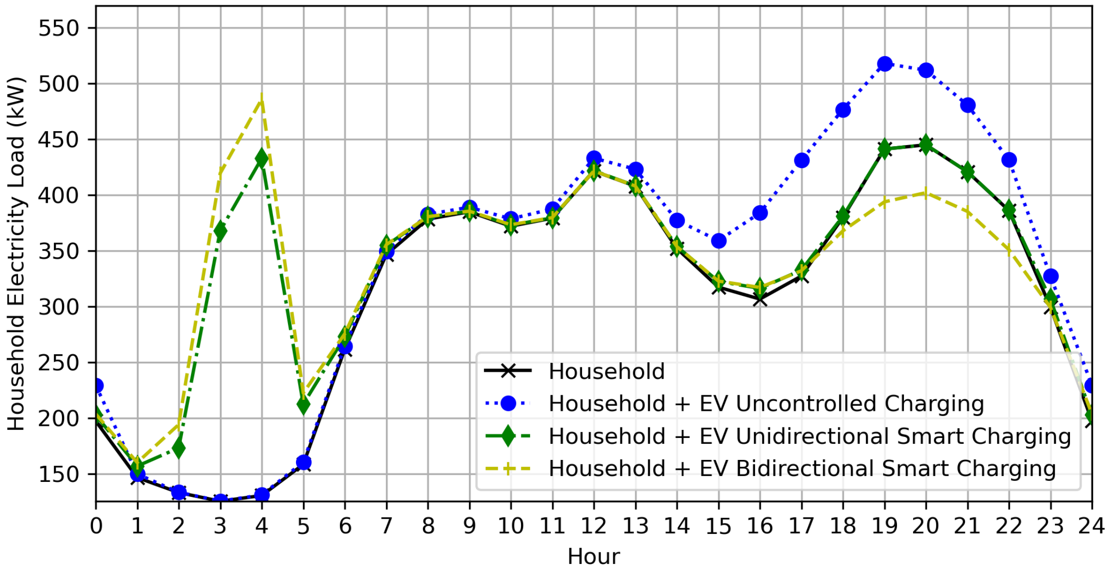

Figure 2. The hourly electricity load profile of the original household, and the original household plus EV uncontrolled charging, EV unidirectional smart charging, and EV bidirectional smart charging with SoC prediction (QRF+Mobility) at 0.75 input quantile.

- **RQ 1.3**: To what extent can next-day prediction help gain monetary benefits and achieve peak-shaving effects?

  In our unidirectional smart charging, there is a trade-off for users between gaining monetary benefits and undertaking the risk of charging outside the home after running out of EV batteries. In general, unidirectional charging helps users gain monetary benefits and shaves the peaks brought by uncontrolled charging with the SoC prediction quantile ≥ 0.5.

  For our bidirectional smart charging, as the input quantile of predictions increases, less risk is undertaken and more benefit is gained, and it results in higher risks and monetary benefits than unidirectional smart charging because of the discharging design. However, this design might lead to the cases that unexpected mobility needs after arriving home can not be fulfilled. As for peak-shaving effects, no extra stress is brought to the original maximum peak when the quantile of SoC prediction is kept below 70%.

Several research directions can be further explored to improve the performance of probabilistic forecasting and enhance the applicability of smart charging in reality. First, other mobility features that can distinguish mode choices and depict traveling habits from the temporal perspective can be examined. Motif, for example, is a mobility feature that describes typical movements by considering the time series of visited locations on a semantic level (Song et al., 2010b; Schneider et al., 2013; Xu et al., 2018). Besides, socio-demographic factors can be considered to model the mobility decision-making behaviors if data are available (Bucher et al., 2020). Second, our current study only considers days with valid energy consumption and parking duration in the forecasting. However, in reality, smart charging should also consider days without valid values. Future research could consider adding the prediction of whether an EV is used on a particular day, whose influencing factors have been discussed in Bucher et al. (Bucher et al., 2020). Third, the simulation of smart charging in our research has not considered renewable energy sources, which has been discussed in Martin et al. (2022). Their study considered photovoltaic power generated from house roofs to charge EVs based on historical EV usage data, which could be combined with the prediction models in our study for future cases.

Overall, this study showed that incorporating individual human mobility features could partially improve the probabilistic forecast of EV energy demand. This conclusion advances our understanding of how to use human mobility in energy forecasting and how probabilistic results could play a role in smart charging.

References

Al-Obaidi, A., Khani, H., Farag, H. E., and Mohamed, M.: Bidirectional smart charging of electric vehicles considering user preferences, peer to peer energy trade, and provision of grid ancillary services, International Journal of Electrical Power & Energy Systems, 124, 106 353, 2021.

Bessa, R. J. and Matos, M. A.: The role of an aggregator agent for EV in the electricity market, 2010.

Bucher, D., Martin, H., Hamper, J., Jaleh, A., Becker, H., Zhao, P., and Raubal, M.: Exploring Factors that Influence Individiduals' Choice Between Internal Combustion Engine Cars and Electric Vehicles, AGILE: GIScience Series, 1, 1–23, 2020.

Cuttone, A., Lehmann, S., and Gonz'alez, M. C.: Understanding predictability and exploration in human mobility, EPJ Data Science, 7, 1–17, 2018.

Ester, M., Kriegel, H.-P., Sander, J., and Xu, X.: A Density-Based Algorithm for Discovering Clusters in Large Spatial Databases with Noise, in: Proceedings of the Second International Conference on Knowledge Discovery and Data Mining, KDD'96, p. 226–231, AAAI Press, 1996.

García-Villalobos, J., Zamora, I., San Martín, J. I., Asensio, F. J., and Aperribay, V.: Plug-in electric vehicles in electric distribution networks: A review of smart charging approaches, Renewable and Sustainable Energy Reviews, 38, 717–731, 2014.

Gonzalez, M. C., Hidalgo, C. A., and Barabasi, A.-L.: Understanding individual human mobility patterns, nature, 453, 779–782, 2008.

Hardman, S., Jenn, A., Tal, G., Axsen, J., Beard, G., Daina, N., Figenbaum, E., Jakobsson, N., Jochem, P., Kinnear, N., et al.: A review of consumer preferences of and interactions with electric vehicle charging infrastructure, Transportation Research Part D: Transport and Environment, 62, 508–523, 2018.

Hilpisch, B.: Construction of a user-level probabilistic forecast of electric vehicle usage, Master's Thesis, ETH Zurich, 2020.

Hong, Y., Xin, Y., Martin, H., Bucher, D., and Raubal, M.: A Clustering-Based Framework for Individual Travel Behaviour Change Detection, in: 11th International Conference on Geographic Information Science (GIScience 2021)-Part II, 2021.

Hu, J., You, S., Østergaard, J., Lind, M., and Wu, Q.: Optimal charging schedule of an electric vehicle fleet, in: 2011 46th International Universities' Power Engineering Conference (UPEC), pp. 1–6, VDE, 2011.

Huber, J., Dann, D., and Weinhardt, C.: Probabilistic forecasts of time and energy flexibility in battery electric vehicle charging, Applied Energy, 262, 114 525, 2020.

Koenker, R. and Bassett Jr, G.: Regression quantiles, Econometrica: journal of the Econometric Society, pp. 33–50, 1978.

Kristoffersen, T. K., Capion, K., and Meibom, P.: Optimal charging of electric drive vehicles in a market environment, Applied Energy, 88, 1940–1948, 2011.

Lopes, J. A. P., Soares, F. J., and Almeida, P. M. R.: Integration of electric vehicles in the electric power system, Proceedings of the IEEE, 99, 168–183, 2010.

Martin, H., Becker, H., Bucher, D., Jonietz, D., Raubal, M., and Axhausen, K. W.: Begleitstudie sbb green class-abschlussbericht, Arbeitsberichte Verkehrs-und Raumplanung, 1439, 2019.

Martin, H., Buffat, R., Bucher, D., Hamper, J., and Raubal, M.: Using rooftop photovoltaic generation to cover individual electric vehicle demand—A detailed case study, Renewable and Sustainable Energy Reviews, 157, 111 969, 2022.

Meinshausen, N. and Ridgeway, G.: Quantile regression forests., Journal of Machine Learning Research, 7, 2006.

Mwasilu, F., Justo, J. J., Kim, E.-K., Do, T. D., and Jung, J.-W.: Electric vehicles and smart grid interaction: A review on vehicle to grid and renewable energy sources integration, Renewable and sustainable energy reviews, 34, 501–516, 2014.

Pappalardo, L., Simini, F., Rinzivillo, S., Pedreschi, D., Giannotti, F., and Barabási, A.-L.: Returners and explorers dichotomy in human mobility, Nature communications, 6, 1–8, 2015.

Pappalardo, L., Vanhoof, M., Gabrielli, L., Smoreda, Z., Pedreschi, D., and Giannotti, F.: An analytical framework to nowcast well-being using mobile phone data, International Journal of Data Science and Analytics, 2, 75–92, 2016.

Restrepo, M., Morris, J., Kazerani, M., and Canizares, C. A.: Modeling and testing of a bidirectional smart charger for distribution system EV integration, IEEE Transactions on Smart Grid, 9, 152–162, 2016.

Rhoades, S. A.: The herfindahl-hirschman index, Fed. Res. Bull., 79, 188, 1993.

Schneider, C. M., Belik, V., Couronné, T., Smoreda, Z., and González, M. C.: Unravelling daily human mobility motifs, Journal of The Royal Society Interface, 10, 20130 246, 2013.

Song, C., Koren, T., Wang, P., and Barabási, A.-L.: Modelling the scaling properties of human mobility, Nature physics, 6, 818–823, 2010a.

Song, C., Qu, Z., Blumm, N., and Barabási, A.-L.: Limits of predictability in human mobility, Science, 327, 1018–1021, 2010b.

Sortomme, E. and El-Sharkawi, M. A.: Optimal charging strategies for unidirectional vehicle-to-grid, IEEE Transactions on Smart Grid, 2, 131–138, 2010.

Sundstrom, O. and Binding, C.: Flexible charging optimization for electric vehicles considering distribution grid constraints, IEEE Transactions on Smart grid, 3, 26–37, 2011.

Susilo, Y. O. and Axhausen, K. W.: Repetitions in individual daily activity–travel–location patterns: a study using the Herfindahl–Hirschman Index, Transportation, 41, 995–1011, 2014.

Teng, F., Ding, Z., Hu, Z., and Sarikprueck, P.: Technical Review on Advanced Approaches for Electric Vehicle Charging Demand Management, Part I: Applications in Electric Power Market and Renewable Energy Integration, IEEE Transactions on Industry Applications, 56, 5684–5694, 2020.

Vandael, S., Claessens, B., Hommelberg, M., Holvoet, T., and Deconinck, G.: A scalable three-step approach for demand side management of plug-in hybrid vehicles, IEEE Transactions on Smart Grid, 4, 720–728, 2012.

Wang, C.-C. and Lee, W.-C.: A simple method to estimate prediction intervals and predictive distributions: summarizing meta-analyses beyond means and confidence intervals, Research Synthesis Methods, 10, 255–266, 2019.

Wei, Z., He, J., and Cai, L.: Admission control and scheduling for EV charging station considering time-of-use pricing, in: 2016 IEEE 83rd Vehicular Technology Conference (VTC Spring), pp. 1–5, IEEE, 2016.

Wu, W., Lin, Y., Liu, R., Li, Y., Zhang, Y., and Ma, C.: Online EV charge scheduling based on time-of-use pricing and peak load minimization: properties and efficient algorithms, IEEE Transactions on Intelligent Transportation Systems, 2020.

Xu, Y., Çolak, S., Kara, E. C., Moura, S. J., and González, M. C.: Planning for electric vehicle needs by coupling charging profiles with urban mobility, Nature Energy, 3, 484–493, 2018.

Yuan, Y. and Raubal, M.: Analyzing the distribution of human activity space from mobile phone usage: an individual and urban-oriented study, International Journal of Geographical Information Science, 30, 1594–1621, 2016.

Yuan, Y., Raubal, M., and Liu, Y.: Correlating mobile phone usage and travel behavior–A case study of Harbin, China, Computers, Environment and Urban Systems, 36, 118–130, 2012.

Zhou, Z., Xu, Z., and Wu, W. B.: Long-term prediction intervals of time series, IEEE transactions on information theory, 56, 1436–1446, 2010.

Appendix A: Appendix

The search spaces of hyperparameters in the cross validation of quantile regression are given in Table A1.

Table A1. The search space of hyperparameters for three models.

Model	Hyperparameter	Search Space
LQR	the regularization constant that multiplies the L1 penalty term	$\text{alpha} = 0.001, 0.01, 0.1, 1, 10, 100, 1000$
QRF	the number of trees	$\text{n\_estimators} = 100, 200, 300$
	the maximum depth of the tree	$\text{max\_depth} = 1, 3, 5, 7, \text{None}$
	the minimum number of samples required to split an internal node	$\text{min\_samples\_split} = 2, 5, 10$
	the minimum number of samples required to be at a leaf node	$\text{min\_sample\_leaf} = 1, 2, 4$
GBQR	the number of boosting stages	$\text{n\_estimators} = 100, 200, 300$
	the maximum depth of individual trees	$\text{max\_depth} = 1, 3, 5, 7$
	the contribution of each tree	$\text{learning\_rate} = 0.1, 0.06, 0.02$
	the fraction of samples to be used for individual base learners	$\text{subsample} = 1.0, 0.8, 0.6$
	the minimum number of samples required to split an internal node	$\text{min\_samples\_split} = 2, 5, 10$
	the minimum number of samples required to be at a leaf node	$\text{min\_sample\_leaf} = 1, 2, 4$